Exploration for Wave Propagation Around Ground Loosening Using Discrete Element Method

Kazuki Kuwashiro[1#], *Reiko* Kuwano[1], and *Masahide* Otusbo[2]

[1]*Institute of Industrial Science (IIS), The University of Tokyo, 4-6-1 Komaba, Meguro-ku, Tokyo, 153-8505, Japan*
[2] *Port and Airport Research Institute, 3-1-1 Nagase, Yokosuka-shi, Kanagawa, 239-0826, Japan*
[#]*Corresponding author: kkuwa39@iis.u-tokyo.ac.jp*

ABSTRACT

Ground loosening and subsurface cavities potentially cause ground cave-ins, even if they are deep in the ground. Loosened soil and cavities, for example, formed by shield tunnel excavation or breakage of underground pipes occur frequently. Recently, ground-penetrating radar method has been utilized to detect subsurface cavities, and studies such as dynamic wave surveys have been considered. However, these methods assume that cavities several meters deep can be detected by surface-based surveys, and do not target loosened soil directly above a deep tunnel. This contribution is a fundamental study aimed at detecting loosening depth in the ground, with the goal of measuring dynamic waves from the inside of a tunnel. To understand wave propagation and particle-scale response around loosened sandy soil, this study adopts the discrete element method (DEM) using cohesionless spherical particles. A series of DEM simulations are performed to understand how dynamic waves propagate or reflect around loosened sandy soil in comparison with dense ground without loosening.

Keywords: wave propagation; loosening; discrete element method; geophysical survey.

1. Introduction

In recent years, a ground cave-in which is a sudden collapse of the ground surface has been occurring in various locations both in Japan and abroad. It is known empirically that cohesionless sandy soils are more prone to cave-ins than plastic fine silt or clayey soil. As a countermeasure, the ground-penetrating radar method has been utilized for detecting subsurface cavities caused by buried pipes, etc., in practice. However, its applicability is limited to the relatively shallow ground about 1.5 m below the ground surface. Although studies using dynamic wave surveys have been considered to detect deeper cavities, they are all targeted at detecting cavities several meters deep by surveying from the ground surface. Furthermore, it is important to detect regions of soil loosening before the formation of underground cavities. However, detecting soil loosening zones seems more difficult than detecting underground cavities.

The ground cave-in accident caused by shield tunnel excavation in Chofu, Japan in 2020 revealed that cave-ins could be triggered by ground loosening or cavities even deep underground. Therefore, this study aims to understand the propagation characteristics of dynamic waves in order to detect ground loosening deep underground from the inside of a tunnel. A series of discrete element method (DEM) simulations is performed to assess the particle-scale response around loosened sandy soil by varying the size of the loosened area and the position of a transmitter.

2. Modelling approach

This study performed DEM simulations using granular LAMMPS software (Plimpton 1995). To understand how dynamic waves propagate or reflect around loosened sandy soil, the present simulation approach broadly follows Nakata et al. (2022) who investigated the wave propagation characteristics around a subsurface cavity. This study builds on an earlier work for laboratory element-scale simulations by Otsubo et al. (2020) where wave reflection characteristics at dense and loose interfaces were investigated. This contribution extends their findings by exploring model-scale responses to understand how dynamic waves propagate or reflect around loosened sandy soil in comparison with dense ground without loosening.

2.1. Ground preparation method

To simplify complicated model test conditions, spherical particles with typical glass bead properties were adopted (Young's modulus: 71.6 GPa, Poisson's ratio: 0.23, and specific gravity: 2.65). The diameters of spherical particles range from 1.4 mm to 2.2 mm, representing a uniformly graded sandy soil. A simplified Hertz-Mindlin contact model without cohesion was adopted to calculate contact responses following the Itasca Consulting Group (2007). In this study, ground samples in dry conditions, where no capillary forces exist, were considered.

To represent the ground preparation method in the model test such as Nakata (2020), air-pluviation process in a dry condition was simulated. The original model

ground samples for the following “patchwork” process were prepared. The base of the ground was modelled as frictionless rigid wall boundary, while periodic boundaries were used in the horizontal (X and Y) directions. Interparticle frictions (μ) of 0.01 and 0.5 were used respectively to create dense and loose ground (hereafter referred to as “dense only” and “loose only”). After the pluviation process, the resultant void ratio (e) values were found to be 0.581 for dense only and 0.726 for loose only, and dry bulk density was 1.68 [g/cm^3] for the former and 1.54 [g/cm^3] for the latter.

Combining parts of dense only and loose only samples, two mixed model grounds (0.7 m in length (X), 0.2 m in height (Z), and 0.02 m in depth (Y)) with a locally loosened area were created as shown in Fig.1. A small gap was provided at the loose-dense boundary, and an additional simulation was performed until the gap was closed and the entire ground reached a static equilibrium, where the μ value was increased to 0.5 for all the particles.

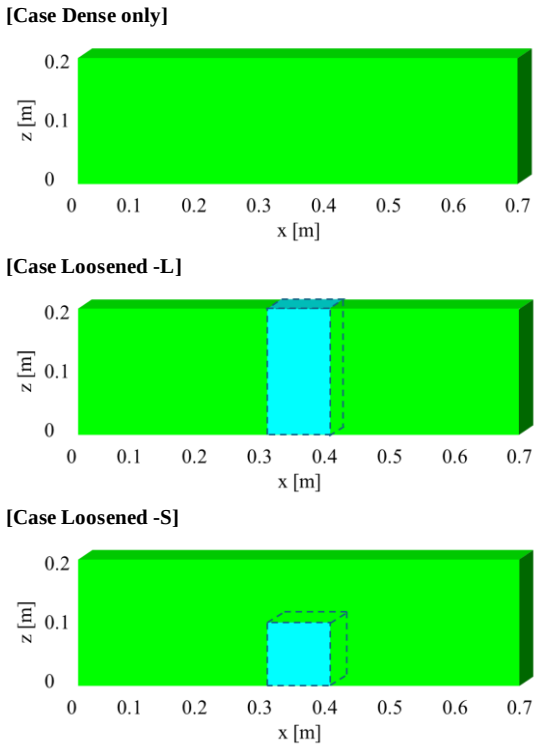

Figure 1. Three ground models for wave propagation simulations. The color of the particles corresponds to the value of friction coefficient (μ), with green indicating a dense area and blue indicating a loose area. Dense ground of the same size without loosening was also prepared for comparison.

2.2. Inter-particle contact forces

The distribution of inter-particle forces in the model grounds with a loosening area was examined prior to performing wave analysis (Fig. 2).

2.2.1. Case Loosened -L

The vertical contact forces are predominant over the horizontal ones due to the effect of gravity. In addition, the magnitude of contact forces appears to be higher in the dense ground due to heavier self-load.

On the other hand, at the boundary between the dense and loose areas, the vertical contact forces are not so strong and the horizontal forces are dominant. This can be understood to be due to arching action, in which soil pressure is exerted to support each other's ground.

2.2.2. Case Loosened -S

Soil arching is generated over the loose area more strongly than Case Loosened -L. This phenomenon can be considered similar to the study that soil surrounding a subsurface cavity becomes loosened, whereas an arch is created over the cavity to support the upper ground in laboratory model tests by Kuwano et al. (2018). Furthermore, Ali et al. (2020) justified that the development of soil arching was able to be discussed even when the periodic boundaries in the horizontal direction were used.

3. Wave propagation simulations

The respective analysis was performed up to the time before the effect of the wave crossing the periodic boundary appeared. To begin, a transmitter is located on the bottom edge in Fig.1 (i.e. at x=0.15[m]) having a region of 0.009 m in length (X), 0.009 m in height (Z), and 0.02 m in depth (Y). The particles inside the region of the transmitter were excited in the X-direction to generate elastic waves, with a single period of cosine wave form (double amplitude displacement: 10 nm; frequency: 1 kHz). Following Otsubo et al. (2020), the μ value was further increased to 0.6 during the wave propagation simulations so that elastic responses of propagating waves can be analysed. Neither local nor viscous damping was used during wave propagation. A dense model ground of the same size without loosening (Case Dense Only) was provided for comparison.

3.1. Wave excitation in the X-direction

Fig. 3 shows time history snapshots of the X-directional particle kinetic energy of the X-excitation for Case Dense Only, Case Loosened -L, and Case Loosened -S model grounds. Note that the selected times for the snapshots are different only in Case Dense Only as the waves propagated faster in the Dense Only ground. For comparison, Fig. 3, etc. shows snapshots of the same wave position instead of the same time: Each snapshot is selected so that the position of the red wave is the same in all cases.

3.1.1. Case Dense only

In the X-excitation, horizontally propagating waves are significantly faster than vertically propagating waves although the stress level is greater at deeper elevations. This phenomenon is considered that shear (S-) waves propagate concentrically towards ground surface, i.e. upwards, but the compression (P-) waves propagate in the X-direction.

3.1.2. Case Loosened -L

In Case Loosened -L, when the wave reaches the boundary between the dense and loose areas, particle

kinetic energy escapes along the boundary in the vertical direction and is not transmitted to the loose area. Otsubo et al. (2020) reported that a granular assembly acts as a lowpass filter against stress/sound waves propagating through the assembly and especially when the waves pass from dense to loose layers as they are rapidly filtered. In model grounds with loosening, the decrease in energy as the wave passes through the loose area is indicative of this filtering effect.

The property of the transmission energy decreasing with each transmission through the boundary, not only from dense to loose but also from loose to dense, can be explained by the concept of acoustic impedance (ZI). In other words, elastic waves have the property of generating reflected waves at the boundary, and the energy of the transmitted waves is taken away by the reflected waves. However, the reflected wave cannot be clearly observed near the boundary in Fig. 3. The reason for this is considered to be the mixing of traveling waves due to excitation and reflected waves from the boundary surface.

3.1.3. Case Loosened -S

In Case Loosened -S, when there are the dense and loose areas in the same direction of wave propagation, the dense one transmits energy faster. This is because P-wave velocity is affected by both the mean coordination number and the stress along its propagation direction, as found in Dutta et al. (2020) and Li et al. (2021). As shown in Fig. 2, the waves can be understood to have propagated along a horizontally stressed soil arch.

When the first traveling wave propagates in the X-direction and transmits through the dense-loose boundary, some of the energy is detached near the bottom and increases a short time later. In all cases, residual energy is observed near the position of the excitation, but it is especially noticeable in Case Loosened -S.

3.2. Wave excitation in the Y-direction

Next, the particles inside the region of the same transmitter were excited in the Y-direction to generate S-waves in both horizontal and vertical directions, with a single period of cosine wave form. Fig. 4 shows time history snapshots of the Y-directional particle kinetic energy of the Y-excitation in each case.

In the Y-excitation case, only S-waves are clearly generated because the excitation is performed perpendicular to the target section, and P- and S-waves are not mixed. In addition, the waves propagate faster in Case Dense Only than in each of the loosened cases. It can be seen that S-waves propagate in concentric circles and are reflected back when they reach the model ground surface. This is considered that the model employed in this study has a two-dimensional structure with a periodically continuous boundary in the depth (Y-) direction, so the energy loss due to excitation is small and the waves oscillated infinitely in the depth direction

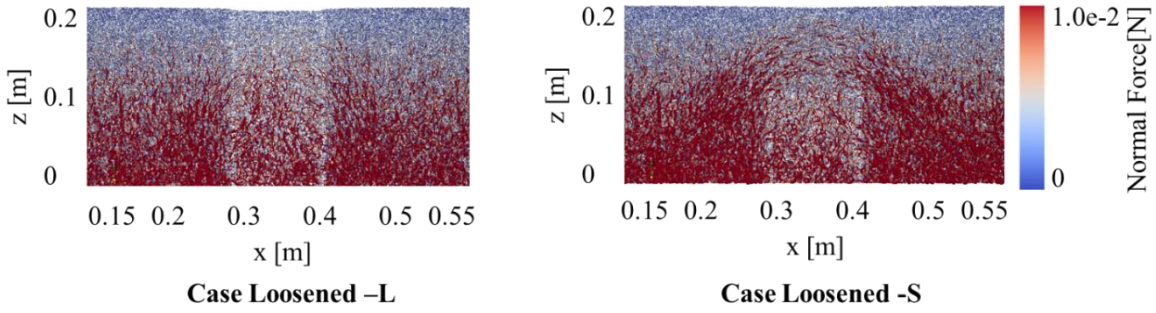

Figure 2. Distribution of inter-particle forces in the model grounds. These images were enlarged in the range of x = 0.15~0.55 [m].

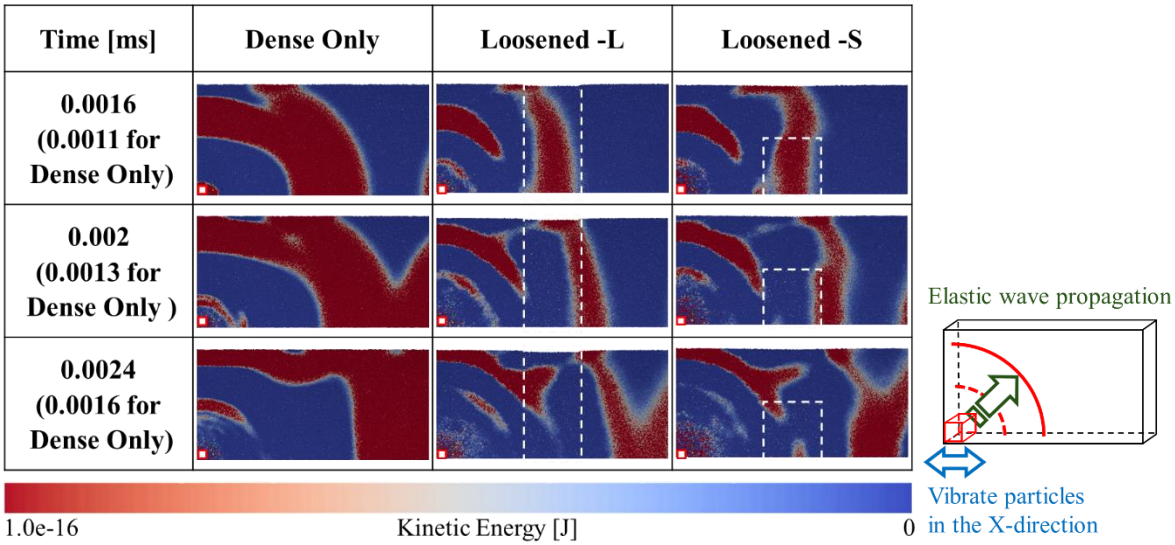

Figure 3. The time history snapshots of the X-directional particle kinetic energy of the X excitation. The transmitter is located on the bottom left (annotated by a square marker). These images were enlarged in the range of x = 0.15~0.55 [m].

(Karasaki, 2022). The energy transmitted through each layer seems to be slightly reduced due to lowpass filtering effects and reflected waves at the boundary.

In Case Loosened -L, the energy of the second traveling S-wave is reduced by transmission through the dense-loose boundary, while in Case Loosened -S it is increased. This is thought to be due to the energy reflected from the upper boundary. In all cases, residual energy is observed near the position of the excitation, but it is especially noticeable in Case Loosened -S.

3.3. Excitation inside loosened area

So far, the wave propagation characteristics have been analyzed by excitation from the dense area. Therefore, the location of the transmitter is changed to the bottom center, i.e. inside the loose area, in order to investigate the difference in wave propagation characteristics. Then, the particles inside the region of the transmitter were excited in the X- or Y-direction to generate P- and S-waves, with a single period of cosine wave form.

Fig. 5 shows time history snapshots of the particle kinetic energy in the X-direction of the X-excitation in each case. Especially in Cases Loosened -L and Loosened -S, residual energy in the bottom loose area can be observed. It is suggested that wave energy may be more likely to remain if there is loosened area near the excitation position. Note that no damping factor was used during wave propagation simulation in this study, and it is only the frictional dissipation that can reduce the excited energy in the system.

Fig. 6 shows time history snapshots of the particle kinetic energy in the Y-direction of the Y-excitation in each case as well. As in Fig. 5, residual energy inside the loose area is observed. In Case Loosened -S, the first traveling S-wave is transmitted, but the second is reflected at the loose-dense boundary. By focusing on the second wave, there is a possibility of capturing the reflected wave at the boundary.

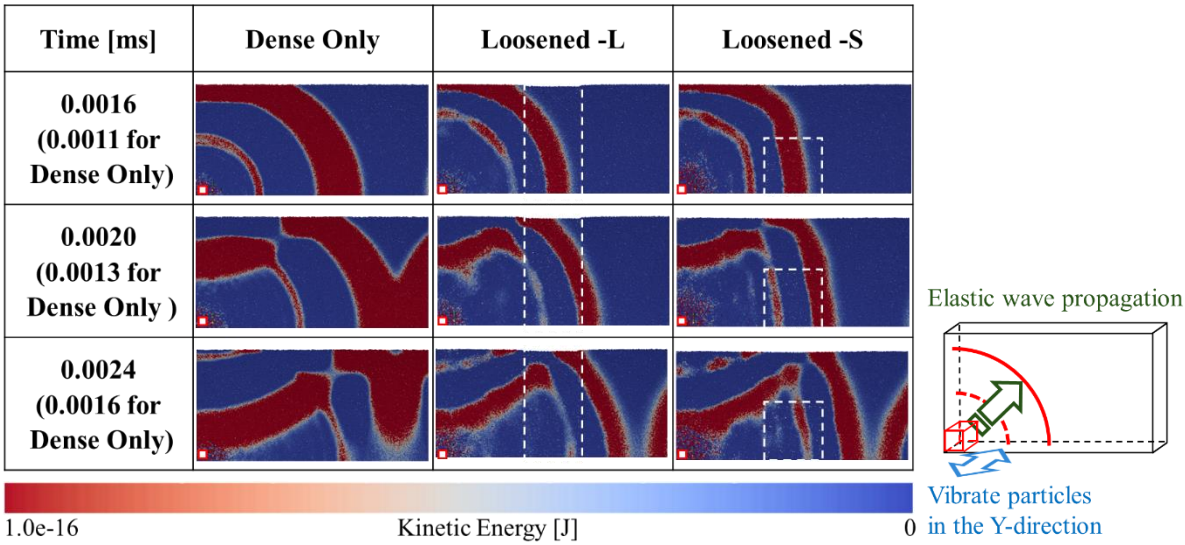

Figure 4. The time history snapshots of the Y-directional particle kinetic energy of the Y excitation. The transmitter is located on the bottom left (annotated by a square marker). These images were enlarged in the range of x = 0.15~0.55 [m].

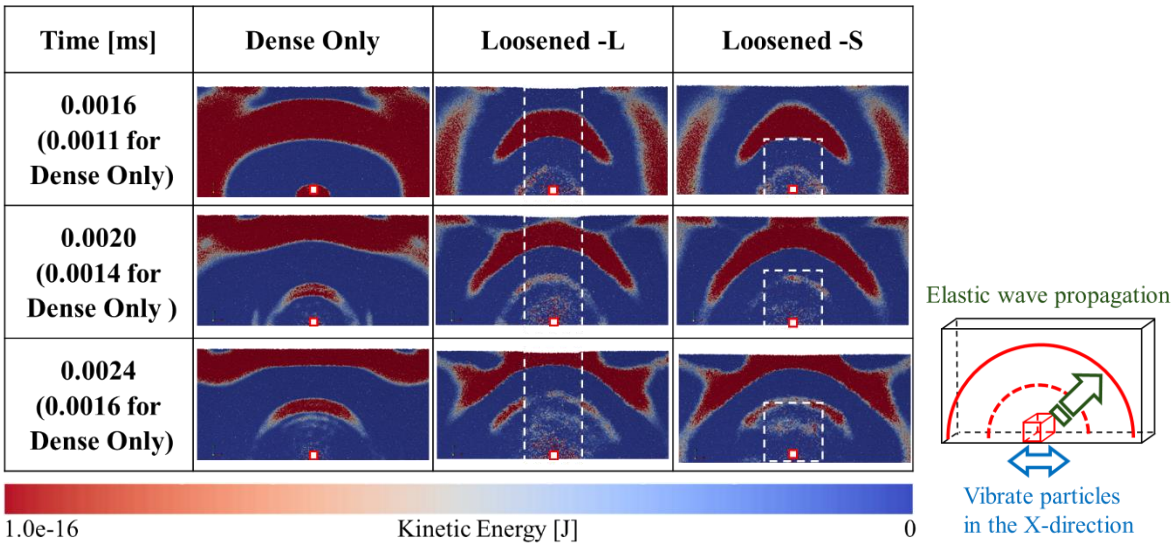

Figure 5. The time history snapshots of the X-directional particle kinetic energy of the X excitation. The transmitter is located on the bottom center (annotated by a square marker). These images were enlarged in the range of x = 0.15~0.55 [m].

4. Conclusions

In this study, wave propagation characteristics around loosened area of ground models were investigated using DEM simulations. The size of loosened area and the location of a transmitter were adjusted according to the features to be extracted. The following main conclusions can be drawn from the comparison with dense ground without loosening.

- When there is dense soil over loosened area, arching contact forces act to support it, and the direction of these forces affects the P-wave velocity, and its propagation direction.
- By observing the particle kinetic energy in the Y-direction of the Y-excitation, the interference of the P-wave signal is reduced and the S-wave propagation characteristics can be analyzed.
- The energy of the wave transmitted through the boundary between dense and loose areas is reduced by the effect of lowpass filtering and reflected waves at the boundary.
- After excitation inside the loosened area, particularly, there is the phenomenon of residual energy in the loosened area, which may be due to reflected waves within loosened area and direct excitation.

In order to detect soil loosening from the inside of a tunnel, further research is needed including verification of the reasons for residual energy and consideration of receivers.

Acknowledgments

This work was supported by Penta-Ocean Construction Co., Ltd. And JSPS KAKENHI Grant Number 22K14322. The simulations presented in this contribution were conducted using the FUJITSU Supercomputer PRIMEHPC FX1000 (Wisteria/BDEC-01) in the Information Technology Center, The University of Tokyo.

References

Ali U., Otsubo M., Ebizuka H. and Kuwano R. “Particle-scale insight into soil arching under trapdoor condition”, Soils and Foundations 60 (5), 1171-1188, 2020. https://doi.org/10.1016/j.sandf.2020.06.011

Dutta T.T., Otsubo M., Kuwano R. and O’Sullivan C. “Evolution of shear wave velocity during triaxial compression”, Soils and Foundations 60 (6), 1357-1370, 2020. https://doi.org/10.1016/j.sandf.2020.07.008

Itasca Consulting Group "PFC3D, version 4.0, User’s manual. Minneapolis”, Itasca (MN, USA), 2007.

Karasaki. “Challenge of detecting deep-ground cavities using wave propagation in soil”, Master thesis, The University of Tokyo, 2022.

Kuwano R., Sera R. and Ohara Y. “Model tests to simulate formation and expansion of subsurface cavities”, Proc. 9th Int'l Conf. on Physical Modelling in Geotechnics, London, 1087-1092, 2018. http://doi.org/10.1201/9780429438646-50

Li Y., Otsubo M. and Kuwano R. “DEM analysis on the stress wave response of spherical particle assemblies under triaxial compression”, Computers and Geotechnics 133, 104043, 2021. https://doi.org/10.1016/j.compgeo.2021.104043

Nakata, Y. "Stress transmission around an underground cavity evaluated using elastic waves", Master thesis, The University of Tokyo, 2020.

Nakata Y., Otsubo M., Ali U. and Kuwano R. “Influence of soil arching and loosening around a subsurface cavity on wave propagation”, 20th International Conference on Soil Mechanics and Geotechnical Engineering, Sydney, 2022.

Otsubo M., Nakata Y. and Kuwano R. “Effect of Locally Loosened Soil on Wave Propagation”, 6th International Conference on Geotechnical and Geophysical Site Characterization, Budapest, 2020. https://doi.org/10.53243/ISC2020-211

Plimpton S. “Fast parallel algorithms for short-range molecular dynamics”, Journal of Computational Physics 117 (1), pp.1-19, 1995. https://doi.org/10.1006/jcph.1995.1039

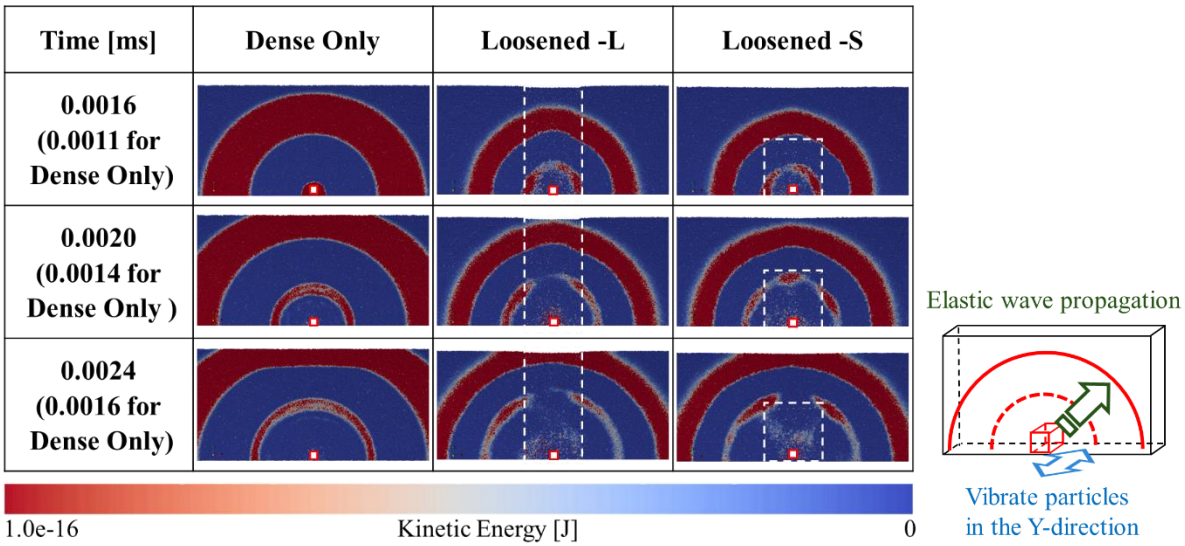

Figure 6. The time history snapshots of the Y-directional particle kinetic energy of the Y excitation. The transmitter is located on the bottom center (annotated by a square marker). These images were enlarged in the range of x = 0.15~0.55 [m].